GSA Data Repository item 0000

Supplemental data for

Exhumation of the West-Central Alborz Mountains, Iran, Caspian Subsidence, and Collision-Related Tectonics

Gary J. Axen, Patrick S. Lam, Marty Grove

Department of Earth and Space Sciences, University of California, Los Angeles

Daniel F. Stockli

Division of Geological and Planetary Sciences, California Institute of Technology, Pasadena

Jamshid Hassanzadeh

Institute of Geophysics, University of Tehran, Iran

Analytical Methods

Mineral Separation Samples were crushed to <600 µm, sized to 30-40 mesh for biotite and K-feldspar and to < 80 mesh for zircon and apatite, and ultrasonically cleaned. Concentrates of zircon, K-feldspar, biotite, and apatite were obtained by standard magnetic and density techniques followed by hand selection under a binocular microscope. The major limitation upon the accuracy of (U-Th)/He age determinations is the potential inclusion of zircon and monazite crystallites that cause irreproducible, anomalously old (U-Th)/He ages (e.g., House et al., 1999). To mitigate against this, each apatite was optically inspected prior to analysis to identify and eliminate inclusion-bearing apatites.

U-Pb Ion Microprobe Analysis The UCLA Cameca ims 1270 ion microprobe was employed to measure U-Pb ages of Au-coated, epoxy-mounted zircons polished to 0.25 µm (Dalyrmple et al., 1999). Lead yields were enhanced by oxygen flooding (3 x 10^{-5} Torr) and a 4-18 nA, 25 µm primary O^- beam. Measurements of ^{208}Pb and ^{232}Th were used to correct for common Pb. Standard zircon AS-3 (1099 Ma; Paces and Miller, 1993) was employed to determine Pb/U relative sensitivity. Corrections for common lead were performed by using ^{208}Pb as a proxy for common Pb after correction for Th-derived ^{208}Pb (see

Compston et al., 1984). Time series analysis indicated that the majority of common Pb originated from surface contamination. Hence we employed anthropogenic Pb compositions from the Los Angeles basin (Sanudo-Wilhelmy and Flegal, 1994) in correcting our results.

^{40}Ar/^{39}Ar Analysis An overview of the ^{40}Ar/^{39}Ar analytical procedures we employed is provided in McDougall and Harrison (1999). Samples were irradiated for 45 hours in the Ford Reactor (L67 position) using Fish Canyon sanidine (27.8±0.3 Ma) to monitor neutron fluence. Step-heating experiments were performed at UCLA in a Ta resistance furnace with the purified gas analyzed by a VG 1200S mass spectrometer (Lovera et al., 1997). Duplicate isothermal measurements were performed at low-temperature to generate the data necessary to correct $^{40}Ar^{*}/^{39}Ar_K$ for Cl-correlated excess ^{40}Ar (Harrison et al., 1994). K-feldspar results were interpreted using the multi-diffusion domain model applied under the constraint of monotonic cooling (Lovera et al., 1997; Quidelleur et al., 1997).

Apatite (U-Th)/He analysis. Helium dating is based on the radiogenic production of ^{4}He from the decay of U and Th (see Hurley, 1954). On geologic time scales, He is completely expelled from apatite above ~80°C, partially retained between ~80-40°C, and totally retained below ~40°C (Farley, 2000; Stockli et al., 2000). Assuming a constant cooling rate of 10°C/my, the (U-Th)/He thermochronometer has a bulk closure temperature of ~70°C. He determinations were carried out at Caltech using noble gas isotope dilution quadruple mass spectrometry. Degassed grains were recovered and dissolved in nitric acid so that their U and Th concentrations could be determined by isotope dilution inductively coupled plasma mass spectrometry. Apparent ages were corrected for alpha loss during decay as described in Farley et al. (1996). Analytical uncertainties on age determinations are generally <6% (±2σ). Multiple experiments were run to determine age reproducibility of individual samples.

References Cited

Compston W., Williams I.S., and Meyer C., 1984, U-Pb geochronology of zircons from Lunar Breccia 73217 using a sensitive, high mass resolution ion microprobe: Proc. 14th Lunar Planet. Sci. Conf. Part 2, Journal of Geophysical Research, v.89, 8525-8534.

Dalrymple, G.B., Grove, M., Lovera, O.M., Harrison, T.M., Hulen, J.B. and Lanphere, M.A., 1999, Age and thermal history of the Geysers Plutonic Complex (Felsite Unit), Geysers Geothermal Field, California: Earth and Planetary Science Letters, v.173, p.285-298.

Farley, K.A., Wolf, R.A., and Silver, L.T., 1996, The effects of long alpha-stopping distances on (U-Th)/He ages: Geochimica et Cosmochimica Acta, v.60, p.4223-4229.

Farley, K. A., 2000, Helium diffusion from apatite; general behavior as illustrated by Durango fluorapatite: Journal of Geophysical Research, v. 105, p. 2903-2914.

Hurley, P.M., 1954, The helium age method and the distribution and migration of helium in rocks. In Nuclear Geology, ed. H. Faul, pp. 301-329. Wiley.

Lovera, O.M., Grove M., Harrison, T.M. and Mahon, K.I., 1997, Systematic analysis of K-feldspar $^{40}Ar/^{39}Ar$ step-heating experiments I: Significance of activation energy determinations: Geochimica et Cosmochimica Acta, v. 61, p. 3171-3192.

McDougall, I. and Harrison, T.M., 1999, Geochronology and Thermochronology Using the $^{40}Ar/^{39}Ar$ Method. Oxford, New York, 269 pp.

Paces, J.B., and Miller, J.D., 1993, Precise U-Pb age of Duluth Complex and related mafic intrusions, northeastern Minnesota: Geochronological insights into physical, petrogenetic, paleomagnetic, and tectonomagmatic processes associated with the 1.1 Ga midcontintent rift system: Journal of Geophysical Research, v.98, p.13,997-14,013.

Quidelleur, X., Grove, M., Lovera, O.M., Harrison, T.M., and Yin, A., 1997, Thermal evolution and slip history of the Renbu Zedong Thrust, southeastern Tibet: Journal of Geophysical Research, v. 102, p. 2659-2679.

Sanudo-Wilhelmy, S.A. and Flegal, A.R. (1994) Temporal variations in lead concentrations and isotopic composition in the Southern California : Geochimica et Cosmochimica Acta, v. 58, p.3315-3320.

Stockli, D. F., Farley, K.A., and Dumitru, T.A., 2000, Calibration of the apatite (U-Th)/He thermochronometer on an exhumed fault block, White Mountains, California: Geology, v. 28, p. 983-986.

Contents of GSA Data Repository item 0000

Item	*PDF file name*
U-Pb data table for Akapol zircon samples (97AK101, 97AK102, and 19-12-1)	Akapol_zircon_data.PDF
U-Pb data table for Alam Kuh zircon samples (19-29-1)	Alam_Kuh_zircon_data.PDF
Concordia plots for all U-Pb samples	Concordia_plots.PDF
$^{40}Ar/^{39}Ar$ data table for 97AK103 K-feldspar (Akapol)	97AK103ksp_data.PDF
Age, Arrhenius, log (r/r_o), and thermal history plots for 97AK103 K-feldspar (Akapol)	97AK103ksp_plots.PDF
$^{40}Ar/^{39}Ar$ data table for 97AK104 K-feldspar (Alam Kuh)	97AK104ksp_data.PDF
Age, Arrhenius, log (r/r_o), and thermal history plots for 97AK104 K-feldspar (Alam Kuh)	97AK104ksp_plots.PDF
$^{40}Ar/^{39}Ar$ data table for 97AK102 biotite (Akapol)	97AK102bio_data.PDF
$^{40}Ar/^{39}Ar$ data table for 97AK103 biotite (Akapol)	97AK103bio_data.PDF
(U-Th)-He data for Akapol and Alam Kuh apatites	Apatite_data.PDF

Ion Microprobe U-Pb results from Alam Kuh zircons

Analysis ID	UO/U[1]	U[2] (ppm)	Th[3] (ppm)	Radiogenic ^{206}Pb[4] (%)	^{206}Pb/^{338}U Age[4] ± 1 σ (Ma)	^{207}Pb/^{335}U Age[5] ± 1 σ (Ma)
19-29-1 zircon						
19-29-1_r1g1s1	8.34	1548	1045	99.8	6.96±0.09	7.4±1.0
19-29-1_r3g1s1	8.21	1515	1739	91.4	6.73±0.14	6.7±2.3
19-29-1_r3g2s1	8.20	854	391	96.4	6.62±0.09	5.6±1.2
19-29-1_r1g2s1	8.28	2326	1392	99.4	6.87±0.08	7.0±0.9
19-29-1_r1g3s1	8.40	2981	2623	99.6	6.96±0.09	7.6±1.3
19-29-1_r3g3s1	8.25	1098	725	98.5	6.61±0.12	6.4±1.5
19-29-1_r1g4s1	8.26	1570	1043	100	6.94±0.08	7.9±1.2
19-29-1_r1g5s1	8.22	467	162	94.5	6.38±0.16	3.7±2.2
19-29-1_r1g6s1	8.17	759	332	97.2	6.55±0.09	5.6±0.9
19-29-1_r1g7s1	8.21	556	535	96.6	6.91±0.22	6.9±2.6
19-29-1_r1g8s1	8.24	3111	1863	98.7	6.99±0.06	6.8±1.0
19-29-1_r1g8s2	8.08	802	445	84.5	6.56±0.21	4.7±4.2
19-29-1_r1g8s3	8.29	798	340	97.5	6.67±0.11	7.1±1.2
19-29-1_r3g5s1	8.70	5495	6582	97.1	6.96±0.22	4.5±2.8

1 Pb/U relative sensitivity calculated from measured UO/U on basis of comparison with AS-3 standard zircon (1099 Ma; Paces and Miller, 1993). Calibration: UO/U = 0.77*(Pb/U) + 4.3 yields 2.75% reproducibility on AS-3 ^{206}Pb/^{238}U ages

2 Estimated by reference to AS-3 zircon (330 ppm U) after normalization by measured $^{94}Zr_2O$.

3 Estimated from measured Th/U using $(Th/U)_{meas}/(Th/U)_{true}$ = 0.85 determined from measurements on AS-3 zircon

4 Calculated using measured ^{208}Pb (corrected for ^{232}Th derived ^{208}Pb) to estimate common ^{206}Pb (^{206}Pb/^{208}Pb = 0.475)

5 Calculated using measured ^{208}Pb (corrected for ^{232}Th derived ^{208}Pb) to estimate common ^{207}Pb (^{206}Pb/^{208}Pb = 0.411)

Ion Microprobe U-Pb results from Akapol zircons

Analysis ID	UO/U[1]	U[2] (ppm)	Th[3] (ppm)	Radiogenic ^{206}Pb[4] (%)	$^{206}Pb/^{338}U$ Age[4] ± 1 σ (Ma)	$^{207}Pb/^{335}U$ Age[5] ± 1 σ (Ma)
97AK102 zircon						
97AK102_A12_1_1	8.91[a]	189	179	65.7	52±5	6±63
97AK102_A12_2_1	8.89[a]	170	119	65.9	59±6	70±63
97AK102_A12_3_1	9.11[a]	302	235	68.8	56±5	54±71
97AK102_A12_4_2	9.04[a]	118	79	66.1	57±5	66±53
97AK102_A12_5_1	8.99[a]	148	104	64.8	61±6	99±74
97AK102_A12_5_2	9.12[a]	216	186	68.2	55±5	78±64
97AK102_A12_8_1	9.11[a]	142	100	65.2	62±5	84±79
97AK102_A12_8_2	9.04[a]	179	127	67.2	54±5	67±71
97AK102_A11_1_1	9.22[a]	228	208	64.6	51±5	60±62
97AK102_A11_3_1	9.20[a]	256	169	63.2	57±5	39±76
97AK102_A11_3_2	9.30[a]	107	52	42.5	52±7	-73±120
97AK102_A11_4_1	9.76[b]	91	72	51.2	62±8	63±98
97AK102_A12_4_3	9.90[b]	125	76	56.4	59±7	72±94
97AK101 zircon						
97AK101_A6_6_1	10.00[b]	270	164	78.4	55±4	43±45
97AK101_A6_7_1	9.78[b]	137	66	61.7	62±8	59±91
97AK101_A6_8_1	9.91[b]	291	210	78.8	59±4	48±43
19-12-1 zircon						
19-12-1_A8_1_1	8.84[a]	196	70	67.4	60±6	44±62
19-12-1_A8_3_1	9.04[a]	390	302	75.6	60±4	66±47
19-12-1_A8_5_1	9.74[a]	600	442	90.2	48±3	65±19

1 Pb/U relative sensitivity calculated from measured UO/U on basis of comparison with AS-3 standard zircon (1099 Ma; Paces and Miller, 1993). Calibration (a): UO/U = 0.27*(Pb/U) + 7.4 yields 1.8% reproducibility on AS-3 $^{206}Pb/^{238}U$ ages; Calibration (b): UO/U = 0.26*(Pb/U) + 8.0 yields 4.6% reproducibility on AS-3 $^{206}Pb/^{238}U$ ages
2 Estimated by reference to AS-3 zircon (330 ppm U) after normalization by measured $^{94}Zr_2O$.
3 Estimated from measured Th/U using $(Th/U)_{meas}/(Th/U)_{true}$ = 0.85 determined from measurements on AS-3 zircon
4 Calculated using measured ^{208}Pb (corrected for ^{232}Th derived ^{208}Pb) to estimate common ^{206}Pb ($^{206}Pb/^{208}Pb$ = 0.475)
5 Calculated using measured ^{208}Pb (corrected for ^{232}Th derived ^{208}Pb) to estimate common ^{207}Pb ($^{206}Pb/^{208}Pb$ = 0.411)

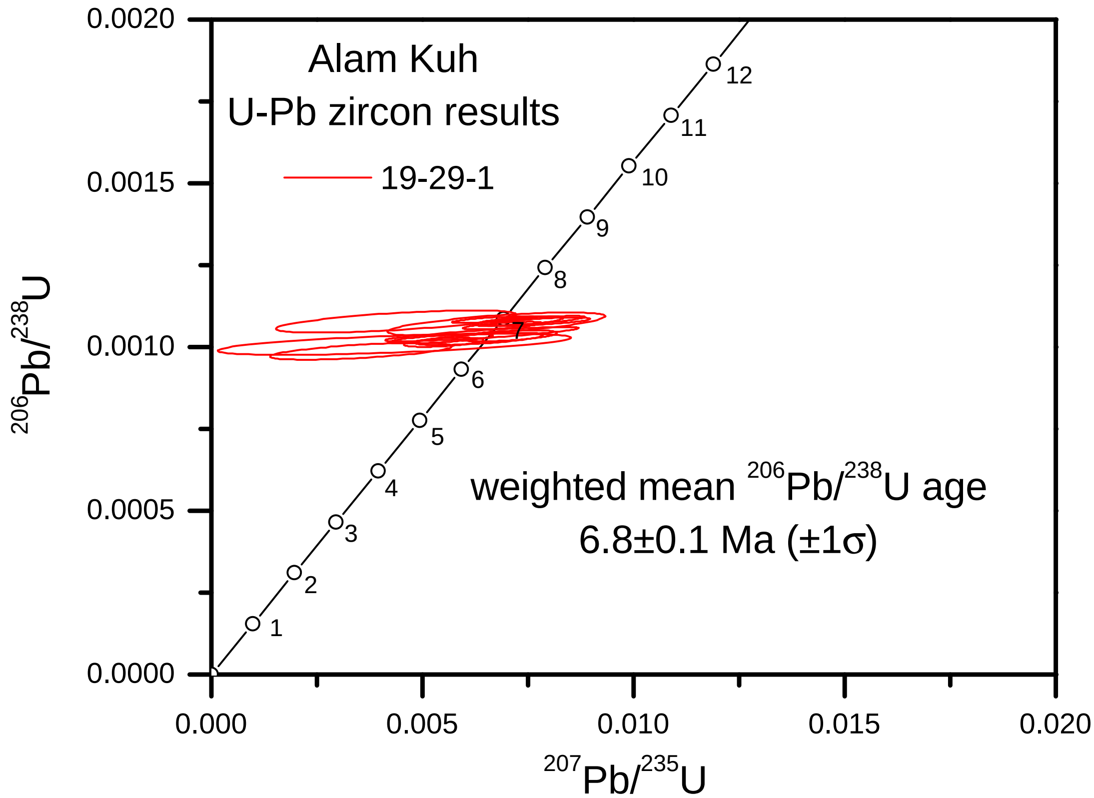
Alam Kuh
U-Pb zircon results
19-29-1
weighted mean $^{206}Pb/^{238}U$ age
6.8±0.1 Ma (±1σ)
$^{206}Pb/^{238}U$
$^{207}Pb/^{235}U$
0.0000
0.0005
0.0010
0.0015
0.0020
0.000
0.005
0.010
0.015
0.020
1
2
3
4
5
6
7
8
9
10
11
12

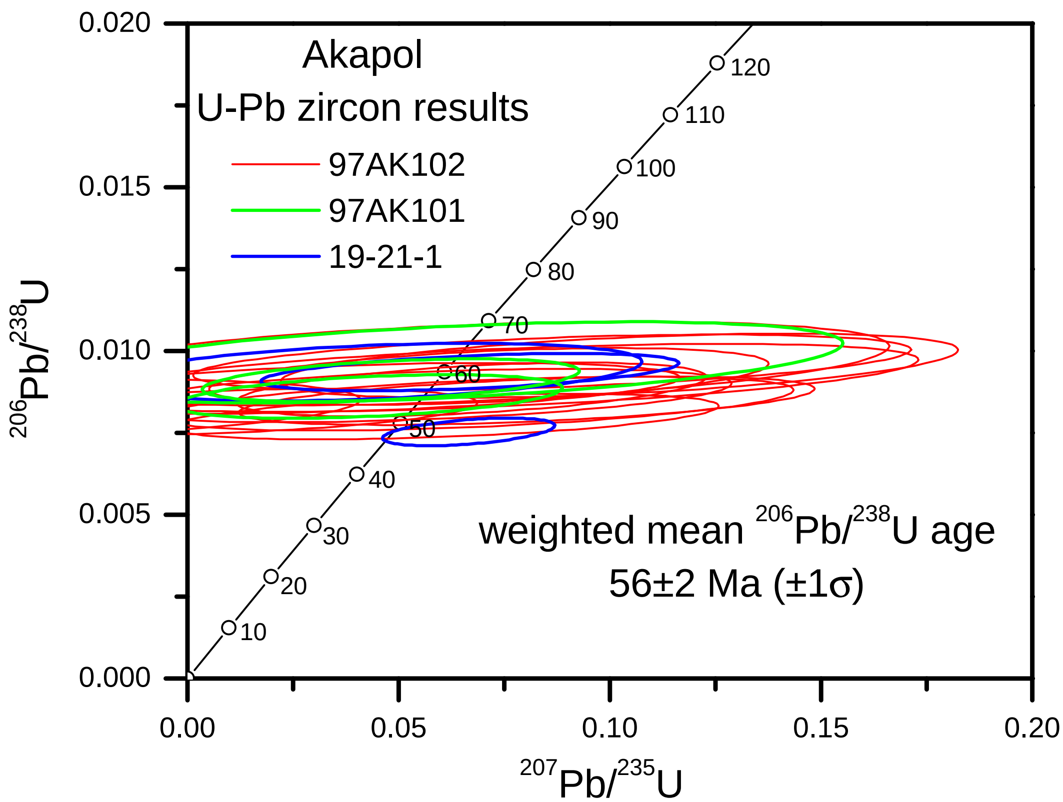
Akapol
U-Pb zircon results
97AK102
97AK101
19-21-1
weighted mean $^{206}Pb/^{238}U$ age
56±2 Ma (±1σ)
$^{206}Pb/^{238}U$
$^{207}Pb/^{235}U$
0.000
0.005
0.010
0.015
0.020
0.00
0.05
0.10
0.15
0.20
10
20
30
40
50
60
70
80
90
100
110
120

97AK103 (Akapol) K-feldspar

	T (°C)	Time (min.)	$^{40}Ar/^{39}Ar$[1] x10^{-1}	$^{38}Ar/^{39}Ar$[1] x10^{-2}	$^{37}Ar/^{39}Ar$[1] x10^{-3}	$^{36}Ar/^{39}Ar$[1] x10^{-4}	$^{39}Ar_K$[2] (mol) x10^{-15}	$^{39}Ar_K$ (%)	$^{40}Ar^*$[3] (%)	$^{40}Ar^*/^{39}Ar_K$[4] ± 1σ x10^{-1}	Cl/K[5] ± 1σ x10^{-3}	Apparent Age[6] ± 1σ (Ma)	Corrected Age[7] ± 1σ (Ma)
1	450	16	952.5	437.3	97.41	1443	2.933	0.1424	55.14	525.9±4.7	1201±4	581±4	0±223
2	450	20	265.4	95.23	50.84	505.7	0.5144	0.1674	42.48	115.7±5.6	257.8±2.1	145±7	0±13
3	500	17	200.9	60.94	47.04	228.4	1.676	0.2488	65.61	133.2±2.1	164.3±0.5	166±3	0±5
4	500	20	104.9	24.19	34.12	140.9	1.408	0.3172	58.77	63.02±1.05	62.96±0.43	80±1	0±2
5	550	17	170.2	25.35	42.96	136.3	5.335	0.5763	75.95	129.8±0.7	66.20±0.48	161.5±0.8	21.41±1.80
6	550	21	53.07	7.000	47.81	47.85	3.619	0.7521	71.74	38.71±0.77	15.82±0.25	49.73±0.97	15.70±1.17
7	600	15	120.6	15.92	59.78	106.6	10.25	1.250	73.52	88.92±0.28	40.22±0.11	112.2±0.3	26.32±0.84
8	600	21	39.43	3.859	71.65	25.38	7.025	1.591	79.52	31.74±0.50	7.234±0.079	40.87±0.64	25.71±0.67
9	650	16	66.31	7.751	89.97	56.45	15.79	2.358	74.33	49.45±0.16	17.85±0.05	63.28±0.20	25.01±0.39
10	650	20	34.07	2.082	79.73	17.16	11.34	2.908	83.82	28.81±0.15	2.355±0.029	37.14±0.19	32.71±0.20
11	700	15	45.88	3.503	91.94	32.54	23.01	4.026	78.38	36.08±0.21	6.211±0.021	46.39±0.27	33.53±0.29
12	700	20	33.99	1.608	90.03	9.461	17.87	4.894	90.71	31.01±0.18	1.082±0.022	39.94±0.23	38.31±0.23
13	750	15	42.26	2.761	119.0	21.98	35.36	6.611	84.05	35.61±0.09	4.211±0.024	45.79±0.12	37.32±0.14
14	750	20	34.52	1.413	113.6	4.591	23.76	7.765	92.47	33.00±0.13	0.569±0.028	42.48±0.17	41.97±0.17
15	800	15	37.31	1.685	138.2	6.942	18.48	8.663	88.74	35.11±0.23	1.309±0.077	45.16±0.29	43.04±0.32
16	800	15	36.80	1.339	128.3	5.234	20.62	9.664	94.87	35.10±0.14	0.361±0.024	45.15±0.17	45.10±0.17
17	500	832	205.9	2.613	107.6	564.5	1.456	9.735	18.72	38.95±2.45	0.978±0.584	50.03±3.10	48.64±3.22
18	800	38	37.06	1.330	115.7	4.468	28.71	11.13	95.72	35.58±0.11	0.339±0.013	45.75±0.14	45.75±0.14
19	825	34	37.80	1.359	114.7	5.443	30.15	12.59	95.07	36.03±0.14	0.413±0.020	46.32±0.17	46.32±0.17
20	850	32	38.10	1.420	105.1	4.851	30.59	14.08	95.54	36.49±0.12	0.586±0.055	46.91±0.16	46.91±0.16
21	875	40	38.56	1.438	91.91	6.033	34.77	15.77	94.69	36.60±0.08	0.629±0.019	47.04±0.10	47.04±0.10
22	900	15	40.41	1.505	83.52	11.61	13.93	16.44	90.53	36.79±0.22	0.786±0.032	47.29±0.28	47.29±0.28
23	925	20	39.15	1.556	77.99	7.244	24.32	17.63	93.73	36.82±0.09	0.949±0.030	47.32±0.11	47.32±0.11
24	950	17	39.63	1.580	65.49	8.964	23.40	18.76	92.49	36.78±0.20	1.007±0.035	47.27±0.25	47.27±0.25
25	975	23	39.13	1.652	53.48	8.018	34.58	20.44	93.19	36.56±0.09	1.211±0.055	46.99±0.12	46.99±0.12
26	1000	15	39.57	1.777	45.53	8.162	23.99	21.61	93.06	36.94±0.11	1.557±0.033	47.48±0.13	47.48±0.13
27	1025	17	39.82	1.895	44.89	8.793	34.03	23.26	92.72	37.01±0.10	1.880±0.042	47.57±0.13	47.57±0.13
28	1050	16	40.34	2.099	49.98	9.188	35.16	24.97	92.54	37.41±0.12	2.443±0.030	48.08±0.15	48.08±0.15
29	1075	15	41.06	2.320	53.60	10.48	39.16	26.87	91.76	37.75±0.08	3.048±0.046	48.51±0.10	48.51±0.10

	T (°C)	Time (min.)	$^{40}Ar/^{39}Ar^{1}$ x10^{-1}	$^{38}Ar/^{39}Ar^{1}$ x10^{-2}	$^{37}Ar/^{39}Ar^{1}$ x10^{-3}	$^{36}Ar/^{39}Ar^{1}$ x10^{-4}	$^{39}Ar_K{}^{2}$ (mol) x10^{-15}	$^{39}Ar_K$ (%)	$^{40}Ar^{*3}$ (%)	$^{40}Ar^*/^{39}Ar_K{}^{4}$ ± 1σ x10^{-1}	Cl/K[5] ± 1σ x10^{-3}	Apparent Age[6] ± 1σ (Ma)	Corrected Age[7] ± 1σ (Ma)
30	1100	15	42.14	2.489	52.12	11.87	45.24	29.07	91.01	38.42±0.09	3.510±0.014	49.36±0.11	49.36±0.11
31	1100	38	41.78	2.370	43.69	11.71	66.47	32.30	91.09	38.10±0.07	3.180±0.017	48.95±0.09	48.95±0.09
32	1100	62	42.09	2.468	41.11	10.32	66.66	35.53	92.13	38.82±0.05	3.461±0.016	49.87±0.06	49.87±0.06
33	1100	120	43.51	2.614	40.33	12.01	81.76	39.50	91.24	39.74±0.04	3.856±0.014	51.03±0.05	51.03±0.05
34	1100	186	45.11	2.763	40.46	13.85	80.03	43.39	90.36	40.80±0.05	4.259±0.027	52.37±0.06	52.37±0.06
35	1100	221	46.63	2.927	40.61	16.02	63.81	46.49	89.28	41.67±0.05	4.701±0.010	53.47±0.07	53.47±0.07
36	1200	17	50.18	4.560	73.12	18.37	92.43	50.98	88.73	44.56±0.06	9.214±0.028	57.12±0.08	57.12±0.08
37	1225	10	48.26	4.046	54.75	12.71	186.6	60.04	91.72	44.29±0.05	7.818±0.014	56.78±0.06	56.78±0.06
38	1250	8	47.02	3.603	38.06	8.362	381.8	78.58	94.21	44.33±0.06	6.614±0.035	56.82±0.08	56.82±0.08
39	1300	10	47.24	3.296	33.97	6.565	306.8	93.48	95.34	45.08±0.05	5.774±0.047	57.78±0.07	57.78±0.07
40	1350	8	55.12	4.786	154.0	29.17	45.90	95.71	84.01	46.37±0.12	9.784±0.030	59.41±0.15	59.41±0.15
41	1650	9	52.44	4.469	192.0	21.60	87.02	99.94	87.56	45.96±0.06	8.948±0.043	58.88±0.08	58.88±0.08
42	1650	7	149.7	6.223	243.9	348.0	1.256	99.99	30.76	46.82±2.45	12.11±0.34	59.97±3.09	59.97±3.09

1 Corrected for backgrounds (mean values in (mol): m/e40 = 4x10^{-16}; m/e39 = 1x10^{-16}; m/e38 = 1.8x10^{-17}; m/e37 = 1.8x10^{-17}; m/e36 = 1.6x10^{-17}), mass discrimination (measured $^{40}Ar/^{36}Ar_{ATM}$ = 296.5±0.5), abundance sensitivity (5 ppm), and radioactive decay (Irradiated: 02/09/2000; Analyzed: 04/13/2000)

2 Normalized to 100% delivery to mass spectrometer

3 Includes static line blank

4 Corrected for atmospheric argon and nucleogenic interferences ($^{40}Ar/^{39}Ar_K$ = 0.025;$^{36}Ar/^{39}Ar_{Ca}$ = 0.00025;$^{39}Ar/^{37}Ar_{Ca}$ = 0.00078)

5 Corrected for atmospheric argon and and nucleogenic interferences and production ratios ($^{38}Ar/^{39}Ar_K$ = 0.012; Cl/K = 0.277 $^{38}Ar_{Cl}/^{39}Ar_K$; $^{36}Cl/^{38}Cl$ = 316)

6 Assumes trapped argon is atmospheric. J-factor = 0.007219 (assumes Fish Canyon sanidine = 27.8 Ma)

7 Corrected for Cl-correlated excess ^{40}Ar ($^{40}Ar_E$; Harrison et al., 1994) using $^{40}Ar_E$ = 1.52±0.01x10^{-5}; Cl/K offset = 3.4x10^{-4}

8 All uncertainties reflect analytical errors only

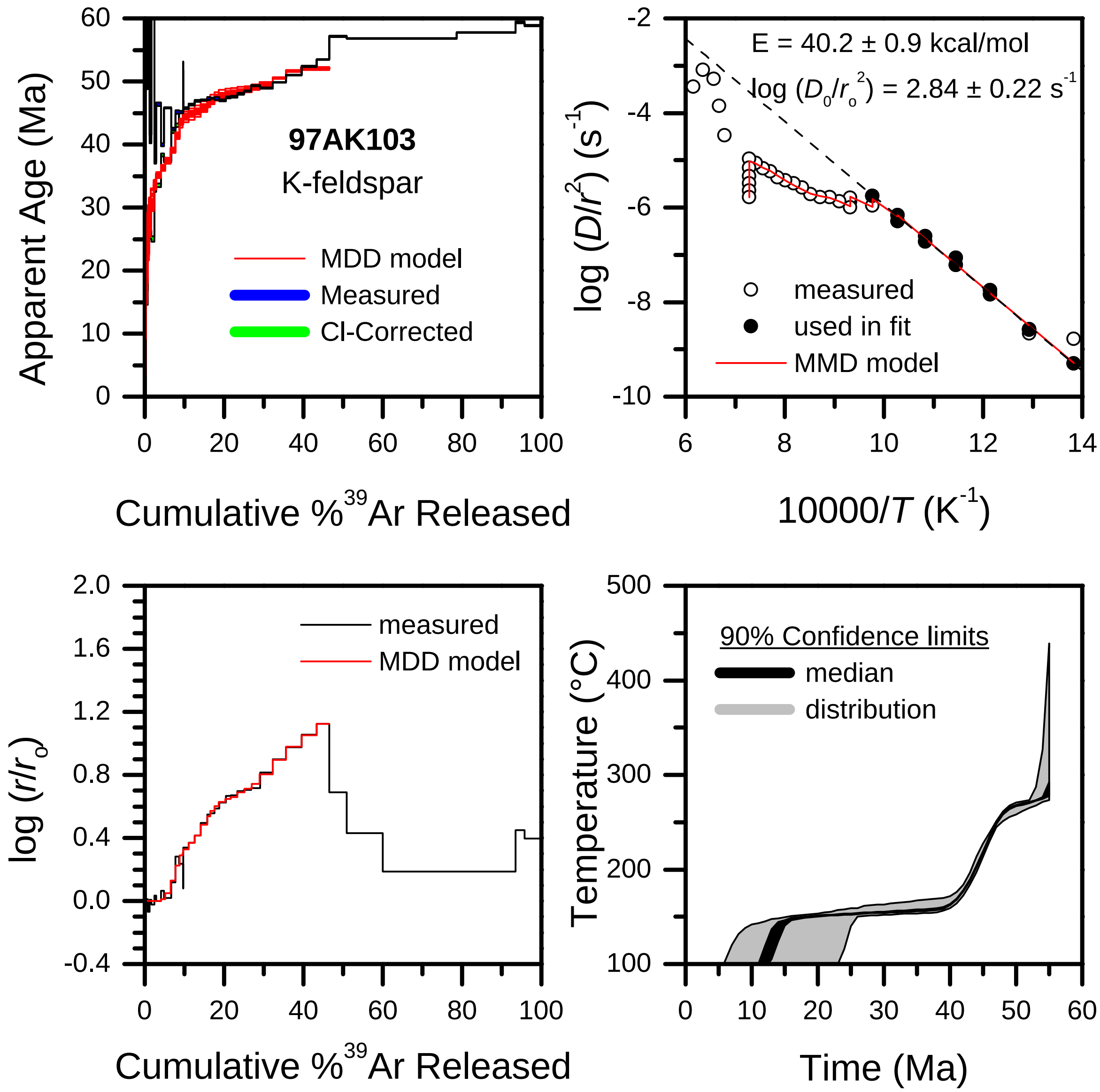
97AK103
K-feldspar
MDD model
Measured
Cl-Corrected
Apparent Age (Ma)
Cumulative %39Ar Released
E = 40.2 ± 0.9 kcal/mol
log (D0/ro2) = 2.84 ± 0.22 s-1
measured
used in fit
MMD model
log (D/r2) (s-1)
10000/T (K-1)
measured
MDD model
log (r/ro)
Cumulative %39Ar Released
90% Confidence limits
median
distribution
Temperature (°C)
Time (Ma)

Alam Kuh sample 97AK104 K-feldspar

	T (°C)	Time (min.)	$^{40}Ar/^{39}Ar$[1]	$^{38}Ar/^{39}Ar$[1] x10^{-2}	$^{37}Ar/^{39}Ar$[1] x10^{-3}	$^{36}Ar/^{39}Ar$[1] x10^{-3}	$^{39}Ar_K$[2] (mol) x10^{-15}	$^{39}Ar_K$ (%)	$^{40}Ar^*$[3] (%)	$^{40}Ar^*/^{39}Ar_K$[4] ± 1σ x10^{-2}	Cl/K[5] ± 1σ x10^{-2}	Apparent Age[6] ± 1σ (Ma)	Corrected Age[7] ± 1σ (Ma)
1	450	14	132.1	565.4	75.71	440.7	4.351	0.1989	1.367	180.7±0.6	154.0±0.4	23±7	13±16
2	450	20	77.21	109.4	9.774	259.8	0.8817	0.2392	0.5486	42.57±0.80	28.62±0.27	6±10	4±11
3	500	15	19.76	67.47	31.46	66.60	2.629	0.3594	0.3039	6.046±0.199	18.01±0.07	1±3	0±3
4	500	22	12.39	28.91	16.99	41.53	2.512	0.4742	0.7126	8.925±0.220	7.458±0.055	1±3	1±3
5	550	15	5.996	15.04	20.80	19.20	6.004	0.7487	4.937	29.89±0.05	3.733±0.020	3.90±0.63	3.64±0.71
6	550	20	3.846	4.403	32.61	11.69	6.253	1.035	9.487	37.02±0.04	0.826±0.008	4.82±0.55	4.77±0.56
7	600	16	3.049	4.444	32.61	8.757	15.61	1.748	14.28	43.86±0.01	0.853±0.008	5.71±0.17	5.66±0.19
8	600	20	1.981	2.047	18.03	5.079	12.80	2.333	22.72	45.61±0.02	0.208±0.010	5.94±0.26	5.93±0.26
9	650	15	2.571	4.258	13.64	6.943	24.14	3.437	19.17	49.57±0.02	0.811±0.003	6.46±0.26	6.40±0.27
10	650	21	1.802	2.053	11.01	4.354	23.29	4.502	27.01	49.07±0.01	0.214±0.004	6.39±0.17	6.38±0.17
11	700	15	2.540	4.165	11.21	6.768	44.19	6.522	20.26	51.61±0.01	0.786±0.005	6.72±0.14	6.67±0.16
12	700	21	1.428	2.228	9.909	2.987	36.20	8.177	36.28	52.13±0.01	0.269±0.015	6.79±0.13	6.77±0.13
13	750	15	1.320	2.541	10.15	2.678	52.73	10.59	38.03	50.42±0.01	0.358±0.002	6.57±0.07	6.55±0.07
14	750	20	0.8363	1.585	9.101	1.019	49.76	12.86	60.57	51.08±0.01	0.101±0.002	6.65±0.12	6.65±0.12
15	800	15	0.7851	1.769	8.830	0.8527	72.34	16.17	64.41	50.88±0.00	0.153±0.001	6.63±0.06	6.62±0.06
16	800	20	0.7280	1.410	7.055	0.6653	59.22	18.88	69.09	50.70±0.00	0.055±0.003	6.60±0.06	6.60±0.06
17	825	20	0.7200	1.528	6.289	0.6277	63.65	21.79	70.30	51.00±0.01	0.088±0.001	6.64±0.09	6.64±0.09
18	850	15	0.7961	1.741	5.954	0.9087	65.41	24.77	62.76	50.31±0.00	0.145±0.004	6.55±0.06	6.55±0.06
19	875	15	0.8194	1.742	5.475	0.9671	70.08	27.98	61.74	50.90±0.00	0.145±0.002	6.63±0.06	6.63±0.06
20	900	16	0.8581	1.811	5.403	1.069	77.66	31.53	60.02	51.78±0.00	0.164±0.001	6.74±0.04	6.74±0.04
21	925	15	1.018	2.043	5.463	1.632	79.44	35.16	49.97	51.08±0.00	0.225±0.003	6.65±0.04	6.65±0.04
22	950	16	1.087	2.196	5.550	1.875	78.67	38.76	46.57	50.86±0.01	0.266±0.001	6.62±0.09	6.62±0.09
23	975	16	1.371	2.704	5.723	2.873	79.69	42.40	36.17	49.78±0.01	0.402±0.002	6.48±0.10	6.48±0.10
24	1000	16	1.559	3.283	6.185	3.435	81.35	46.12	33.23	51.96±0.01	0.559±0.002	6.77±0.07	6.77±0.07
25	1000	55	1.390	3.400	6.296	2.885	114.8	51.36	36.84	51.32±0.00	0.594±0.002	6.68±0.05	6.68±0.05
26	1025	15	1.708	4.490	6.106	3.890	36.37	53.03	31.11	53.44±0.01	0.891±0.005	6.96±0.18	6.96±0.18
27	1050	15	1.948	5.598	6.957	4.822	52.50	55.43	25.50	49.83±0.01	1.193±0.003	6.49±0.11	6.49±0.11
28	1075	15	1.839	6.379	8.503	4.431	69.45	58.60	27.42	50.56±0.01	1.412±0.007	6.59±0.07	6.59±0.07
29	1100	16	1.860	7.824	10.07	4.484	92.54	62.83	27.38	51.03±0.01	1.812±0.008	6.65±0.08	6.65±0.08

	T (°C)	Time (min.)	$^{40}Ar/^{39}Ar$[1]	$^{38}Ar/^{39}Ar$[1] x10^{-2}	$^{37}Ar/^{39}Ar$[1] x10^{-3}	$^{36}Ar/^{39}Ar$[1] x10^{-3}	$^{39}Ar_K$[2] (mol) x10^{-15}	$^{39}Ar_K$ (%)	$^{40}Ar^*$[3] (%)	$^{40}Ar^*/^{39}Ar_K$[4] ± 1σ x10^{-2}	Cl/K[5] ± 1σ x10^{-2}	Apparent Age[6] ± 1σ (Ma)	Corrected Age[7] ± 1σ (Ma)
30	1100	33	1.738	7.187	10.72	4.087	95.24	67.18	29.05	50.59±0.00	1.637±0.005	6.59±0.05	6.59±0.05
31	700	921	16.18	9.412	10.68	52.59	2.402	67.29	3.760	61.23±0.20	2.001±0.027	7.97±2.57	7.97±2.57
32	1100	76	1.230	4.723	10.09	2.398	70.38	70.51	40.32	49.76±0.01	0.963±0.005	6.48±0.14	6.48±0.14
33	1100	165	1.496	5.783	11.16	3.256	80.38	74.19	33.99	50.97±0.01	1.253±0.003	6.64±0.10	6.64±0.10
34	1200	18	1.817	9.040	14.04	4.338	240.5	85.18	28.11	51.12±0.01	2.149±0.006	6.66±0.11	6.66±0.11
35	1225	11	1.688	7.485	13.85	3.870	107.9	90.11	30.78	52.03±0.01	1.721±0.002	6.78±0.11	6.78±0.11
36	1250	15	1.713	7.382	16.06	3.920	112.9	95.27	30.94	53.07±0.01	1.692±0.003	6.91±0.07	6.91±0.07
37	1300	15	1.689	7.351	45.29	3.839	42.93	97.23	31.43	53.31±0.01	1.684±0.009	6.94±0.13	6.94±0.13
38	1350	19	1.949	7.880	53.71	4.654	33.68	98.77	28.24	55.29±0.01	1.826±0.007	7.20±0.18	7.20±0.18
39	1650	11	3.777	7.826	23.99	10.72	26.41	99.98	15.49	58.68±0.02	1.780±0.008	7.64±0.23	7.64±0.23
40	1650	14	153.2	21.32	16.12	512.0	0.4023	99.99	1.240	191.0±3.2	2.909±0.139	24.75±41.00	24.75±41.00

1 Corrected for backgrounds (mean values in (mol): m/e40 = 2.2x10^{-16}; m/e39 = 6.7x10^{-17}; m/e38 = 2.3x10^{-17}; m/e37 = 1.8x10^{-17}; m/e36 = 2.1x10^{-17}), mass discrimination (measured $^{40}Ar/^{36}Ar_{ATM}$ = 296.5±0.5), abundance sensitivity (5 ppm), and radioactive decay (Irradiated: 02/09/2000; Analyzed: 04/10/2000)

2 Normalized to 100% delivery to mass spectrometer

3 Includes static line blank

4 Corrected for atmospheric argon and nucleogenic interferences ($^{40}Ar/^{39}Ar_K$ = 0.025;$^{36}Ar/^{39}Ar_{Ca}$ = 0.00025;$^{39}Ar/^{37}Ar_{Ca}$ = 0.00078)

5 Corrected for atmospheric argon and and nucleogenic interferences and production ratios ($^{38}Ar/^{39}Ar_K$ = 0.012; Cl/K = 0.277 $^{38}Ar_{Cl}/^{39}Ar_K$; $^{36}Cl/^{38}Cl$ = 316)

6 Assumes trapped argon is atmospheric. J-factor = 0.007232 (assumes Fish Canyon sanidine = 27.8 Ma)

7 Corrected for Cl-correlated excess ^{40}Ar ($^{40}Ar_E$; Harrison et al., 1994) using $^{40}Ar_E$ = 5±6x10^{-8}; Cl/K offset = 5.5x10^{-4}

8 All uncertainties reflect analytical errors only

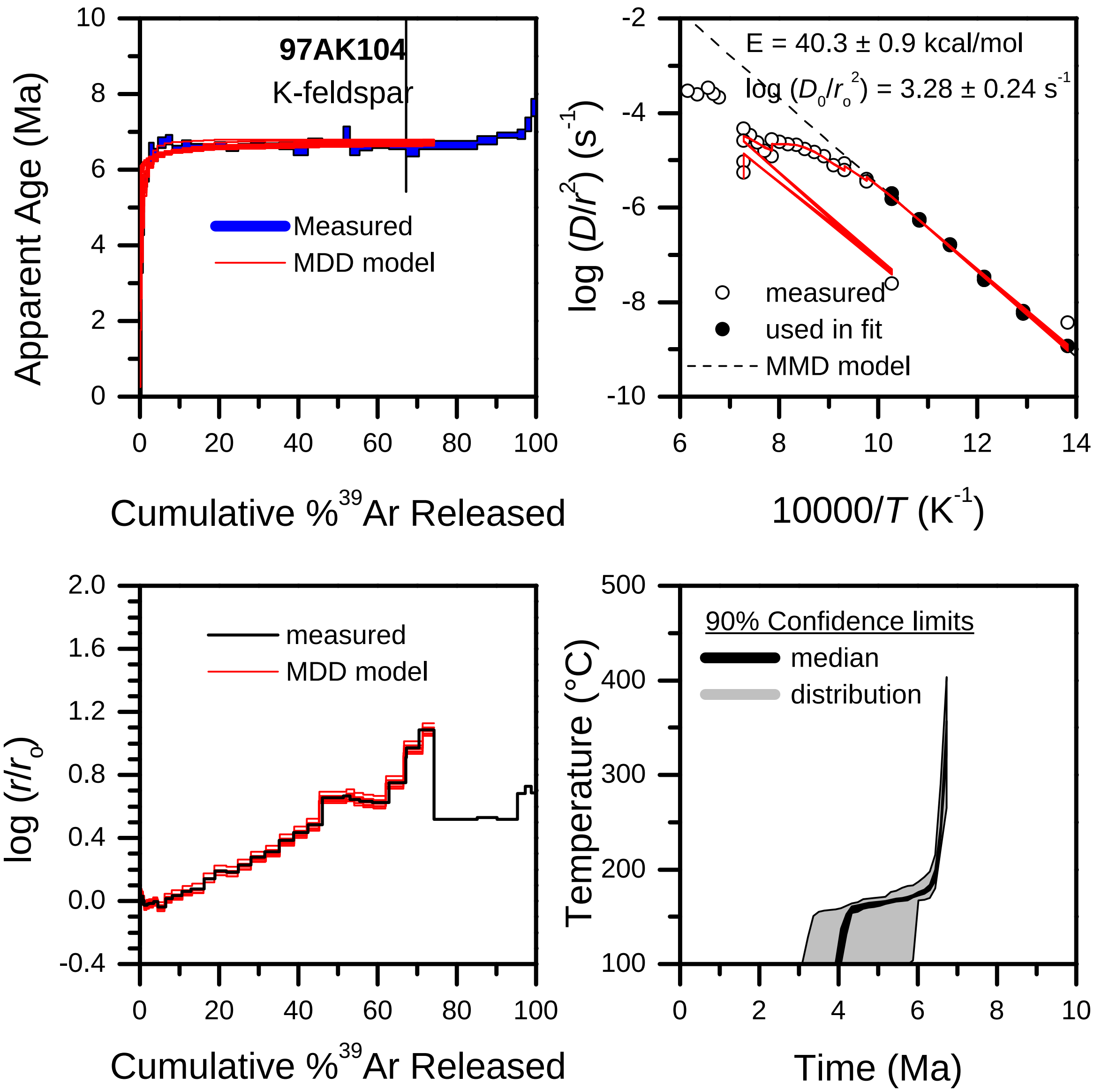
97AK104
K-feldspar
Measured
MDD model
Apparent Age (Ma)
Cumulative %39Ar Released
E = 40.3 ± 0.9 kcal/mol
log (D0/ro2) = 3.28 ± 0.24 s-1
measured
used in fit
MMD model
log (D/r2) (s-1)
10000/T (K-1)
measured
MDD model
log (r/ro)
Cumulative %39Ar Released
90% Confidence limits
median
distribution
Temperature (°C)
Time (Ma)

97AK102 (Akapol) biotite

	T (°C)	Time (min.)	$^{40}Ar/^{39}Ar$[1]	$^{38}Ar/^{39}Ar$[1] x10^{-2}	$^{37}Ar/^{39}Ar$[1] x10^{-3}	$^{36}Ar/^{39}Ar$[1] x10^{-3}	$^{39}Ar_K$[2] (mol) x10^{-15}	$^{39}Ar_K$ (%)	$^{40}Ar*$[3] (%)	$^{40}Ar*/^{39}Ar_K$[4] ± 1σ x10^{-1}	Apparent Age[5] ± 1σ (Ma)	$^{39}Ar_K/^{40}Ar$[6] ± 1σ x10^{-2}	$^{36}Ar/^{40}Ar$[6] ± 1σ x10^{-5}
1	500	196	106.5	299.1	229.3	346.7	1.989	0.2401	3.779	40.30±6.69	51.86±8.49	0.9392±0.0027	325.6±2.1
2	600	10	12.24	12.27	339.9	30.84	0.8226	0.3395	24.85	31.31±4.65	40.41±5.93	8.184±0.019	251.7±12.9
3	700	10	6.671	13.86	124.8	11.32	7.240	1.213	49.30	33.09±0.41	42.68±0.52	15.05±0.04	169.9±1.9
4	780	10	6.284	17.19	12.44	6.397	30.87	4.941	69.43	43.69±0.10	56.16±0.12	15.98±0.02	102.2±0.4
5	850	10	4.713	17.21	5.929	0.9915	76.07	14.12	93.19	43.95±0.06	56.48±0.07	21.33±0.02	21.12±0.24
6	900	10	4.749	17.17	6.815	1.005	45.47	19.61	93.11	44.28±0.07	56.90±0.09	21.17±0.02	21.23±0.44
7	950	10	4.823	17.14	8.358	1.199	34.47	23.77	91.99	44.44±0.09	57.10±0.12	20.84±0.01	24.95±0.63
8	1000	10	4.857	17.27	18.10	1.166	36.67	28.20	92.27	44.89±0.13	57.67±0.16	20.70±0.04	24.03±0.60
9	1050	10	4.928	17.66	27.60	1.289	35.12	32.44	91.65	45.24±0.07	58.11±0.09	20.40±0.02	26.14±0.38
10	1100	10	4.776	17.58	26.14	0.8923	58.44	39.50	93.90	44.90±0.05	57.68±0.06	21.05±0.01	18.64±0.26
11	1200	10	4.535	17.41	29.56	0.3073	340.6	80.61	97.37	44.21±0.07	56.81±0.09	22.17±0.02	6.651±0.478
12	1350	17	4.742	17.93	88.21	0.9875	158.6	99.75	93.39	44.32±0.06	56.94±0.07	21.20±0.02	20.47±0.26
13	1350	13	20.01	18.18	107.9	53.06	2.059	100	21.39	43.10±4.15	55.41±5.25	5.004±0.011	265.4±7.0

1 Corrected for backgrounds (mean values in (mol): m/e40 = 1.9x10^{-16}; m/e39 = 3.5x10^{-17}; m/e38 = 1.1x10^{-17}; m/e37 = 1.1x10^{-17}; m/e36 = 1.0x10^{-17}), mass discrimination (measured $^{40}Ar/^{36}Ar_{ATM}$ = 296.5±0.5), abundance sensitivity (5 ppm), and radioactive decay (Irradiated: 02/09/2000; Analyzed: 05/02/2000)

2 Normalized to 100% delivery to mass spectrometer

3 Includes static line blank

4 Corrected for atmospheric argon and nucleogenic interferences ($^{40}Ar/^{39}Ar_K$ = 0.025; $^{36}Ar/^{39}Ar_{Ca}$ = 0.00025; $^{39}Ar/^{37}Ar_{Ca}$ = 0.00078)

5 Assumes trapped argon is atmospheric. J-factor = 0.007236 (assumes Fish Canyon sanidine = 27.8 Ma)

6 Corrected for static line blank and nucleogenic interferences

97AK103 (Akapol) biotite

	T (°C)	Time (min.)	$^{40}Ar/^{39}Ar^{1}$ x10^{-1}	$^{38}Ar/^{39}Ar^{1}$ x10^{-2}	$^{37}Ar/^{39}Ar^{1}$ x10^{-3}	$^{36}Ar/^{39}Ar^{1}$ x10^{-3}	$^{39}Ar_K{}^{2}$ (mol) x10^{-15}	$^{39}Ar_K$ (%)	$^{40}Ar^{*3}$ (%)	$^{40}Ar^*/^{39}Ar_K{}^{4}$ ± 1σ x10^{-1}	Apparent Age[5] ± 1σ (Ma)	$^{39}Ar_K/^{40}Ar^{6}$ ± 1σ x10^{-2}	$^{36}Ar/^{40}Ar^{6}$ ± 1σ x10^{-4}
1	500	32	226.6	193.0	111.3	74.01	4.815	0.5601	3.395	7.711±1.397	10.04±1.81	4.418±0.018	32.69±0.21
2	600	14	108.8	12.24	65.41	32.65	5.456	1.195	11.12	12.16±0.93	15.81±1.20	9.208±0.013	30.05±0.29
3	700	26	72.60	9.529	29.68	14.20	27.87	4.436	41.83	30.41±0.28	39.27±0.35	13.82±0.02	19.62±0.13
4	780	21	56.62	9.108	13.67	5.083	55.74	10.92	72.98	41.36±0.11	53.20±0.13	17.74±0.02	9.012±0.051
5	850	31	55.37	9.050	16.05	3.798	75.89	19.75	79.25	43.91±0.13	56.43±0.17	18.14±0.01	6.884±0.079
6	900	10	55.68	9.071	15.51	3.604	28.78	23.09	80.30	44.79±0.06	57.54±0.07	18.04±0.00	6.496±0.035
7	950	10	54.24	8.995	20.15	3.162	38.58	27.58	82.23	44.66±0.09	57.38±0.12	18.52±0.01	5.848±0.056
8	1000	12	54.99	9.182	39.53	3.382	70.79	35.81	81.36	44.78±0.06	57.53±0.07	18.27±0.01	6.161±0.028
9	1100	14	53.55	9.450	134.6	2.992	178.6	56.59	83.16	44.56±0.08	57.25±0.10	18.76±0.01	5.551±0.046
10	1350	18	49.00	9.108	107.7	1.343	373.3	99.99	91.50	44.87±0.04	57.64±0.05	20.51±0.01	2.700±0.015

1 Corrected for backgrounds (mean values in (mol): m/e40 = $1.8x10^{-16}$; m/e39 = $3.6x10^{-17}$; m/e38 = $1.2x10^{-17}$; m/e37 = $1.1x10^{-17}$; m/e36 = $1.0x10^{-17}$), mass discrimination (measured $^{40}Ar/^{36}Ar_{ATM}$ = 296.5±0.5), abundance sensitivity (5 ppm), and radioactive decay (Irradiated: 02/09/2000; Analyzed: 05/02/2000)

2 Normalized to 100% delivery to mass spectrometer

3 Includes static line blank

4 Corrected for atmospheric argon and nucleogenic interferences ($^{40}Ar/^{39}Ar_K$ = 0.025; $^{36}Ar/^{39}Ar_{Ca}$ = 0.00025; $^{39}Ar/^{37}Ar_{Ca}$ = 0.00078)

5 Assumes trapped argon is atmospheric. J-factor = 0.007236 (assumes Fish Canyon sanidine = 27.8 Ma)

6 Corrected for static line blank and nucleogenic interferences

Apatite (U-Th)/He results from the Alam Kuh area, Northern Iran

Sample	He ID	Raw Age (Ma)	Corrected Age (Ma)	U (ppm)	Th (ppm)	He (nmol/g)	Mass (mg)	FT*	Radius (μm)	Length (μm)	Inclusions
19-9-1a	00GF1	3.6	*4.9*	25.1	112.6	1.01	29.4	0.73	44.2	249.5	no
19-9-1b	00GF2	3.4	*4.8*	28.3	132.5	1.11	26.8	0.72	42.5	229.5	no
19-29-1a	00BF1	12.4	*17.1*	13.3	98.7	2.45	25.9	0.72	44.0	204.8	yes (bad)
19-29-1b	00BF2	8.3	*9.9*	10.7	109.7	1.65	44.5	0.85	80.4	302.7	yes
19-29-1c	00BF3	9.2	*12.7*	11.7	78.3	1.51	14.4	0.73	39.0	212.1	yes (bad)
19-29-1d	00GN1	5.5	*7.6*	17.0	76.2	1.05	18.8	0.73	43.5	182.7	no
19-29-1e	00GN2	12.7	*17.0*	13.4	98.2	2.52	23.9	0.75	43.0	226.0	yes (bad)
19-31-1a	00GE1	7.0	*8.9*	13.0	69.2	1.12	18.9	0.79	52.3	182.6	yes
19-31-1b	00GE2	5.9	*7.3*	12.2	76.6	0.97	27.9	0.80	48.6	213.3	no
19-79-2a	00GZ1	6.2	*7.7*	21.5	203.7	2.33	25.7	0.80	44.4	239.4	no
19-79-2b	00GZ2	5.8	*7.5*	21.6	206.5	2.22	30.6	0.78	43.3	209.6	no
19-80-1a	00GC1	11.1	*15.8*	13.2	105.4	2.30	16.7	0.70	38.3	259.9	no
19-80-1b	00GC2	17.0	*23.9*	12.1	83.1	2.92	14.3	0.71	42.0	184.5	yes (bad)
19-106-1a	00GB1	4.3	*6.1*	19.2	61.9	0.78	17.9	0.71	41.4	194.4	no
19-106-1b	00GB2	3.7	*5.5*	25.5	74.9	0.88	16.6	0.67	36.3	195.8	no
19-106-2b	00GM1	4.8	*6.9*	47.6	111.3	1.93	14.5	0.70	39.0	194.0	no
19-106-2b	00GM2	3.5	*5.0*	46.8	101.7	1.33	15.4	0.70	40.0	198.0	yes
19-106-3a	00GD1	3.5	*5.2*	57.6	60.6	1.38	14.3	0.68	37.1	171.0	no
19-106-3b	00GD2	3.3	*4.8*	58.7	64.2	1.32	17.3	0.68	37.8	187.5	no
97AK102a	00BD1	3.5	*4.5*	90.7	51.4	1.95	46.5	0.78	55.9	273.8	no
97AK102b	00BD2	3.0	*4.4*	72.8	34.4	1.31	16.9	0.69	37.3	181.4	no
97AK103a	00BE1	4.3	*5.2*	49.4	93.7	1.69	88.0	0.84	74.8	412.4	no
97AK103b	00BE2	3.5	*4.4*	70.3	208.3	2.25	49.4	0.79	60.5	247.5	no
97AK104a	00HA1	16.8	*21.3*	11.9	121.5	3.70	63.5	0.79	56.1	268.6	yes (bad)
97AK104b	00HA2	15.2	*19.8*	8.3	57.3	1.79	40.0	0.77	50.5	229.5	no

* Fraction of alpha particles retained, as calculated using the technique described by Farley et al., 1996.